Two-vibron state dynamics in an anharmonic confined adlayer

V. Pouthier and C. Girardet
Laboratoire de Physique Moléculaire, UMR CNRS 6624. Faculté des Sciences-La Bouloie, Université de Franche-Comté, 25030 Besançon cedex, France

(Received 30 July 2001; published 27 December 2001)

The two-vibron dynamics of an anharmonic molecular monolayer confined between surface steps is investigated. Using the number states method, the equivalence between the two-vibron dynamics and the dynamics of a single fictitious particle moving in a three-dimensional lattice is established. This latter lattice contains local defects which characterize both the influence of the confinement and the effect of the anharmonicity, and give rise to localized states. The anharmonicity is responsible for the occurrence of localized two-vibron bound states, for which two quanta are located on the same molecule adsorbed close to the surface step. These states are more strongly localized than the corresponding single-vibron states. In addition, the sensitivity of the spectral response of the two-vibron states to the structure and the confinement size is demonstrated using a limited set of dynamical parameters (anharmonicity, lateral hopping constant, and internal vibration frequency). As a result, two-vibron spectroscopy appears as a powerful tool to investigate the growth of molecular monolayers adsorbed on stepped surfaces.

DOI: 10.1103/PhysRevB.65.035414 PACS number(s): 03.65.Ge, 63.22.+m, 63.20.Pw, 63.20.Ry

I. INTRODUCTION

The creation of low-dimensional atomic or molecular devices, which are able to transfer information at the nanometer scale, constitutes one of the challenges of the modern technology. In this context, surfaces exhibiting self-organized defects play a key role in the formation of nanostructures with a well-defined geometry. As an example, vicinal surfaces show regularly arranged steps that are ideal templates for the formation of one-dimensional wires or two-dimensional confined monolayers.[1–3] The interest in adsorbed layers for the nanotechnology is still reinforced by the use of local probes (scanning tunneling microscopy, atomic force microscopy,...), which can serve as tools to build nanostructures by manipulating the adsorbate or inducing chemical reactions[4–8] and to excite the electronic and vibrational degrees of freedom of the admolecules.[9]

Recently, it has been suggested that the transfer of information in molecular nanostructures can be achieved using the collective internal vibrations of the admolecules.[10,11] Indeed, the coupling between the internal degrees of freedom of the admolecules through the lateral interaction favors the coherent propagation of the internal vibrations from one molecule to another yielding the formation of vibrons. However, using vibrons as a vehicle for the information transfer is subjected to two related conditions. The first condition is the confinement of the vibrational energy inside the nanostructure without dramatic energy losses over relatively long times. The second condition is the fabrication of nanosystems with well-defined geometry and size able to prevent these energy losses. Although the formation of vicinal surfaces on metal surfaces has reached a high level of sophistication, it is well-known that the vibron dynamics exhibits a fast energy relaxation due to resonances between the vibron energies and the continuum of electron-hole pair excitations. By contrast, ionic and semiconductor substrates appear to be good candidates since the energy relaxation occurs via multiphonon excitations, which require in general much longer lifetimes. A remarkable example is given by the lifetime of the stretching vibration of CO on NaCl which was measured to be about 10 ms.[12] Recently, it has been demonstrated that ionic vicinal surfaces can be obtained from epitaxial growth of NaCl films on vicinal Ge(100) or Al(111) substrates[13] and we can expect the creation of low-dimensional layers on such stepped surfaces. Another example is given by the hydrogen-terminated vicinal Si surfaces,[14–17] which exhibit a well-defined geometry and offer a good compromise for the vibron lifetime [about 1 ns at 300 K (Ref. 18)].

In a two-dimensional periodic and infinite molecular monolayer, vibrons are Bloch waves characterized by a two-dimensional wave vector, which propagate freely inside the layer. However, the confinement of the monolayer modifies the nature of both vibrons[11] and phonons.[19,20] First, the finite size of the adlayer yields the quantization of the wave vector component perpendicular to the confinement direction due to the reflections of the vibronic waves on both sides. Then, the internal frequencies of the molecules adsorbed close to the steps are either redshifted or blueshifted with respect to their values on the terrace. This frequency shift is responsible for the occurrence of localized states described by a wave function which is delocalized along the direction parallel to the steps and strongly localized along the finite size direction.

The previous results, obtained within the harmonic approximation, were therefore restricted to single-vibron states, only. However, the intramolecular anharmonicity is usually non-negligible with respect to the lateral coupling and play a key role in the localization of the vibrational energy as well as in energy transport in both classical and quantum lattices. In classical lattices, the one-site anharmonicty leads to a nonlinear dynamics usually described by the nonlinear Schrödinger equation, which exhibits solitary wave-type solutions such as the Davydov's soliton in one dimension.[21] Another remarkable feature given by this equation is the occurrence of intrinsic localized modes or discrete breathers (for a recent

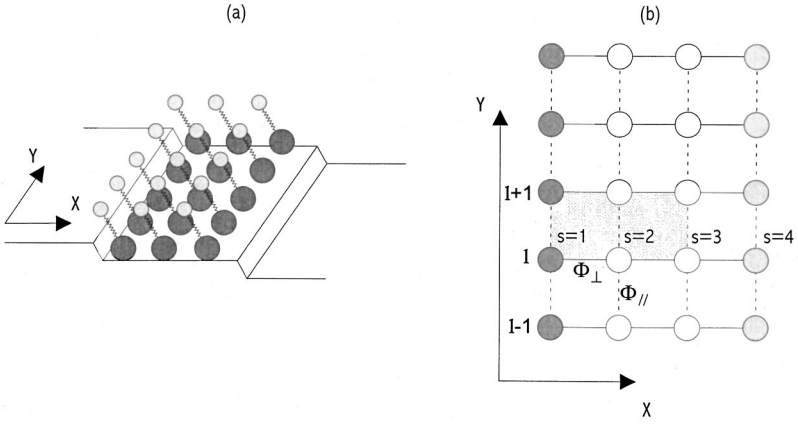

FIG. 1. (a) Molecular monolayer adsorbed on a vicinal surface. The molecules form a periodic lattice along the Y direction parallel to the steps. The unit cell contains N_1 molecules along the X direction perpendicular to the steps. (b) The singularity of the molecule-surface interaction leads to the discrimination between the core molecules (empty circles) adsorbed on the terrace and the sides molecules (gray circle) adsorbed close to the steps. $\Phi_\perp$ is the hopping constant between nearest neighbor molecules belonging to the same unit cell and $\Phi_\parallel$ between nearest neighbor molecules belonging to adjacent cells. $\Phi_\perp$ is used as frequency unit.

review, see for instance Ref. 22) which are not restricted to one-dimensional lattices and correspond to quite general and robust solutions.[23] In quantum lattices, the intramolecular anharmonicity is responsible for the interaction between the vibrons, which favors the formation of bound states.[24] More precisely, when two vibrons are excited, a bound state corresponds to the trapping of two quanta over only a few neighboring molecules with a resulting energy which is lesser than the energy of two quanta lying far apart. The lateral interaction yields a motion of such a state from one molecule to another, thus leading to the formation of a delocalized wave packet with a well-defined momentum. As a result, these bound states can be viewed as the quantum counterpart of breather or soliton excitations[25] and may play an important role in information transfer in a confined molecular monolayer.

In two-dimensional molecular adsorbates, the formation of two-vibron bound states was observed in several systems such as H/Si(111) (Ref. 26) and H/C(111) (Ref. 27) using nonlinear sum frequency generation spectroscopy and CO/Ru(100) using infrared absorption spectroscopy.[28] Bound states in the system H/Ni(111) were investigated using high resolution electron energy loss spectroscopy.[29] In addition, on the basis of examples representative of one, two-dimensional and intermediate cases of lateral coupling, Jakob[30] has demonstrated very recently the powerfulness of two-vibron excitation infrared spectroscopy in probing the density of states of vibrational bands. He has shown that the spectrum contains sufficient information to derive the dimensionality of an adsorbate and to extract the values of the vibrational anharmonicity.

The goal of the present paper is to investigate the two-vibron dynamics in an anharmonic molecular monolayer adsorbed on a stepped surface. A general formalism is introduce to express the Schrödinger equation of the two-vibron states and a Green function calculation is performed to characterize the signature of both the anharmonicity and the confinement on the spectral response of the two-vibron excitations. This latter is determined on the basis of a reduced set of parameters connected to the confinement size, the intramolecular anharmonicity, the internal frequency shift induced by molecular adsorption close to the steps, and the lateral hopping constants between molecules. Then, the question is opened about the molecular information (dynamical interaction process between admolecules and between the molecules and the surface) that could be extracted from the comparison of the details of experimental spectra with the theoretical spectral response.

The paper is organized as follows. In Sec. II, the model for the confined layer and the Hamiltonian of the vibrons are described. In Sec. III, we first introduce the number states method and build the Schrödinger equation for the two-vibron states. Then, the equivalence between the two-vibron dynamics and the motion of a single fictitious particle in a three-dimensional lattice is established. This equivalence is finally used to determine the two-vibron Green function, which allows us to calculate the spectral response. In Sec. IV, some properties of the two-vibron states are presented and they are discussed in Sec. V.

II. MODEL AND HAMILTONIAN

Let us consider a set of $M=N_1\times N_2$ molecules adsorbed on a terrace of a well-defined stepped surface (Fig. 1). These molecules are confined between two parallel and infinite surface steps defining the terrace width and they are assumed to form an ordered monolayer with a square or rectangular structure. This structure is periodic along the Y direction parallel to the steps (periodicity N_2a_2) while along the X direction each unit cell l contains N_1 molecules labeled $s=1,...,N_1$ (size of confinement N_1a_1).

To characterize the internal dynamics of the monolayer, we assume that each molecule (l,s) behaves as an internal oscillator described by the standard creation and annihilation operators b_{ls}^+ and b_{ls}. The (ls)th molecule interacts with the surrounding molecules and with the substrate, leading to a mixing of the internal and external degrees of freedom of the whole system ''monolayer+substrate.'' The Hamiltonian for the whole system can be written in an improved way using the rotating wave approximation (RWA) and the renormalization procedure detailed in Refs. 32 and 33. When the dynamical coupling between the internal and external motions is disregarded, the Hamiltonian which describes the collective dynamics of the internal vibrations is expressed as (using the convention $\hbar=1$)

$$H=\sum_{ls} h_{ls}+\sum_{ls,l's'} \Phi(ls,l's')b_{ls}^+b_{l's'}, \qquad (1)$$

where h_{ls} defines the internal vibration Hamiltonian of the (ls)th molecule renormalized by the static influence of its surrounding and $\Phi(ls,l's')$ represents the lateral dynamical coupling between the internal coordinates at the quadratic order. To minimize the number of parameters, we consider interactions between nearest neighbor molecules and define the hopping constant $\Phi_\perp$ between adjacent molecules belonging to the same unit cell, and the hopping constant $\Phi_\parallel$ between molecules belonging to adjacent unit cells. Note that long range lateral interactions may affect the two-vibron dynamics by inducing changes in the vibron dispersion curves and could modify the formation of localized states. However, these processes are disregarded in the present work. The internal vibration Hamiltonian h_{ls}, including the intramolecular anharmonicity of each molecule, is described according to the model of Kimball *et al.*[24] In this model, the intramolecular potential is expanded up to the fourth order with respect to the internal coordinate and a unitary transformation is performed to keep the vibron-conserving terms, only. The resulting Hamiltonian H is essentially a Bose version of the Hubbard model with attractive interactions, which has demonstrated its usefulness to study molecular vibrations in one-dimensional chains and molecular crystals.

For a confined monolayer, H is expressed as

$$H=\sum_{ls}\ (\omega_s b_{ls}^{+}b_{ls}-Ab_{ls}^{+}b_{ls}^{+}b_{ls}b_{ls})$$

$$+\sum_{ls,l's'}\Phi(ls,l's')b_{ls}^{+}b_{l's'}, \qquad (2)$$

where ω_s stands for the renormalized internal frequency of the (ls)th molecule and A denotes the positive anharmonic parameter due to both the intrinsic anharmonicity of each oscillator and the renormalization of the internal vibration by the interaction with the substrate. The confinement is responsible for a discrimination between the side molecules $s=1$ and N_1, and the core molecules $s=2,...,N_1-1$, which do not experience the same surrounding. To account for this effect, we assume that the renormalization acts differently on the side and core molecules and write the internal frequency as

$$\omega_s=\omega_0+(\omega_1-\omega_0)\delta_{s,1}+(\omega_{N_1}-\omega_0)\delta_{s,N_1}, \qquad (3)$$

where ω_0 is the internal frequency of every core molecule while ω_1 and ω_{N_1} stand for the frequencies of the side molecules. Note that we assume that the anharmonicity is the same for the core and the side molecules.

III. THEORETICAL BACKGROUND

A. Representation of the two-vibron states

The number states method[25] is used to characterize the two-vibron states of the confined monolayer. In a general way, the vibrational quantum states of the (ls)th single molecule can be described by the usual number states $|n_{ls}\rangle$ connected to the eigenvectors of the local number operator $b_{ls}^{+}b_{ls}$. To represent the Hamiltonian H [Eq. (2)], a general orthonormal basis is constructed using the Mth tensor product of these single molecule number states. Since H commutes with the operator $N=\Sigma_{ls}b_{ls}^{+}b_{ls}$ which counts the total number of vibrational quanta, it is possible to find simultaneously eigenstates of both operators. Therefore, the Hilbert space E of the vibrational states can be written as the tensor product $E=E_0\otimes E_1\otimes E_2\otimes\cdots\otimes E_p\cdots$, where E_p denotes the subspace containing the eigenvectors of N associated to the eigenvalue p, namely, the subspace connected to the presence of p vibrational quanta in the confined monolayer. The dimension of E_p is equal to the number of ways of distributing p indistinguishable quanta onto M molecules, i.e., $(p+M-1)!/p!(M-1)!$. Within this representation, the Hamiltonian appears as block-diagonal, each block corresponding to a particular number of vibrational quanta.

In this paper, we focus our attention on the two quanta states belonging to the subspace E_2 with dimension $M(M+1)/2$. A useful basis set to generate the E_2 subspace can be constructed by applying two creation operators on the vacuum state $|0\rangle$ as

$$|l_1,s_1;l_2,s_2)=\left[1-\delta_{l_1l_2}\delta_{s_1s_2}\left(1-\frac{1}{\sqrt{2}}\right)\right]b_{l_1s_1}^{+}b_{l_2s_2}^{+}|0\rangle, \qquad (4)$$

where the factor in the right-hand side of Eq. (4) is a normalization coefficient. To avoid counting twice the vectors $|l_1,s_1;l_2,s_2)$ due to the indistinguishable character of the vibrational quanta, the following restrictions are applied to the numbers l and s: $l_2\geqslant l_1$; when $l_2=l_1$, s_1 varies from 1 to N_1 and $s_2\geqslant s_1$, whereas when $l_2>l_1$, s_1 and s_2 vary independently both from 1 to N_1.

B. The Schrödinger equation

The most general two vibron eigenstate of the Hamiltonian can be expanded as a linear combination of the previous basis vectors as

$$|\Psi\rangle=\sum_{l_1s_1}\sum_{l_2s_2}\Psi(l_1,s_1;l_2,s_2)|l_1,s_1;l_2,s_2). \qquad (5)$$

The expression of the corresponding time independent Schrödinger equation $H|\Psi\rangle=\omega|\Psi\rangle$ depends on the nature of the basis vectors involved in. Indeed, there are two different kinds of basis vectors either describing two quanta located onto molecules which are far apart or two quanta located onto the same molecule.

In the first situation $(l_2>l_1+1)$, the Schrödinger equation is written as

$$[\omega_{s_1}+\omega_{s_2}-\omega+\Phi_\parallel(\Delta_{l_1}+\Delta_{l_2})$$

$$+\Phi_\perp(\Delta_{s_1}+\Delta_{s_2})]$$

$$\times\Psi(l_1,s_1;l_2,s_2)=0, \qquad (6)$$

where Δ_i denotes the discrete Laplacian operator which acts on the ith freedom, i.e., $\Delta_i\Psi(g,h,i,j)=\Psi(g,h,i+1,j)+\Psi(g,h,i-1,j)$. Note that the finite size of the system along X is implicitly taken into account in Eq. (6) by setting to zero the wave function when s_1 or s_2 lie outside the range $[1;N_1]$. Since Eq. (6) involves quanta which are located far from each other, it does not depend on the anharmonic pa-

rameter. This is no longer the case when $l_2=l_1$. For $s_1=s_2=s$ the Schrödinger equation becomes

$$[2\omega_s-2A-\omega]\Psi(l_1,s;l_1,s)+\sqrt{2}\Phi_{\parallel}[\Psi(l_1,s;l_1+1,s)+\Psi(l_1-1,s;l_1,s)]+\sqrt{2}\Phi_{\perp}[\Psi(l_1,s-1;l_1,s)+\Psi(l_1,s;l_1,s+1)]=0, \quad (7)$$

whereas, for $s_2>s_1$, it is expressed as

$$\begin{aligned}[\omega_{s_1}+\omega_{s_2}-\omega]\Psi(l_1,s_1;l_1,s_2)&+\Phi_{\parallel}[\Psi(l_1,s_1;l_1+1,s_2)+\Psi(l_1-1,s_1;l_1,s_2)]\\&+\Phi_{\parallel}[\Psi(l_1,s_2;l_1+1,s_1)+\Psi(l_1-1,s_2;l_1,s_1)]\\&+\Phi_{\perp}[\Psi(l_1,s_1;l_1,s_2+1)+\Psi(l_1,s_1-1;l_1,s_2)]\\&+(1+(\sqrt{2}-1)\delta_{s_2,s_1+1})\Phi_{\perp}[\Psi(l_1,s_1+1;l_1,s_2)\\&+\Psi(l_1,s_1;l_1,s_2-1)]=0. \quad (8)\end{aligned}$$

Note that the Schrödinger equation for $l_2=l_1+1$ can be constructed straightforwardly from [Eqs. (6)–(8)] since the Hamiltonian H is Hermitian.

From a topological point of view, the Schrödinger equation [Eqs. (6)–(8)] is equivalent to the Schrödinger equation for a single particle moving in a four-dimensional hypercubic lattice. This dimension $D=4$ is equal to the number of quanta (i.e., 2) times the Euclidian dimension of the confined monolayer (i.e., 2). However, this dimension D can be reduced to 3 by taking advantage of the periodicity of the confined monolayer along the Y direction. Indeed, since the wave function $\Psi(l_1,s_1;l_2,s_2)$ is invariant with respect to a translation along this direction, it depends on l_1 and $m=l_2-l_1$, and it can be written as a Bloch wave, as

$$\Psi(l_1,s_1;l_2,s_2)=\frac{1}{\sqrt{N_2}}\sum_k \Psi_k(s_1,s_2,m)e^{ik(l_1+l_2)/2}. \quad (9)$$

The total momentum k of the two-vibron states is associated to the motion of the center of mass of the two quanta along Y. The values of k are determined by imposing periodic boundary conditions to the wave function over a set of N_2 unit cells. The resulting wave function $\Psi_k(s_1,s_2,m)$ refers to the degree of freedom m which characterizes the reduced distance between the two vibronic excitations. Note that the previous periodic boundary conditions lead to limit the values taken by the index m which cannot exceed the half size of the periodic box and thus varies from 0 to $(N_2-1)/2$.

Applying the Bloch transformation to Eq. (6) leads to

$$[\omega_{s_1}+\omega_{s_2}-\omega+\tilde{\Phi}_{\parallel}(k)\Delta_m+\Phi_{\perp}(\Delta_{s_1}+\Delta_{s_2})]\Psi_k(s_1,s_2;m)=0, \quad (10)$$

where $\tilde{\Phi}_{\parallel}(k)=2\Phi_{\parallel}\cos(k/2)$. Note that this equation is satisfied for $m>1$, only. In a similar way, Eqs. (7) and (8) are expressed as

$$[2\omega_{s_1}-2A-\omega]\Psi_k(s,s;0)+\sqrt{2}\tilde{\Phi}_{\parallel}(k)\Psi_k(s,s,1)+\sqrt{2}\Phi_{\perp}[\Psi_k(s-1,s;0)+\Psi_k(s,s+1;0)]=0 \quad (11)$$

and

$$\begin{aligned}[\omega_{s_1}+\omega_{s_2}-\omega]\Psi_k(s_1,s_2;0)&+\tilde{\Phi}_{\parallel}(k)[\Psi_k(s_1,s_2;1)+\Psi_k(s_2,s_1;1)]\\&+\Phi_{\perp}[\Psi_k(s_1,s_2+1;0)+\Psi_k(s_1-1,s_2;0)]\\&+[1+(\sqrt{2}-1)\delta_{s_2,s_1+1}]\\&\times\Phi_{\perp}[\Psi_k(s_1,s_2-1;0)+\Psi_k(s_1+1,s_2;0)]=0. \quad (12)\end{aligned}$$

Equations (10)–(12) clearly indicate how the physics of the two vibron states is related to the dynamics of a fictitious single particle moving quantum mechanically inside a three-dimensional lattice. This lattice, shown in Fig. 2(a), appears as a discrete, finite size rod with a length which extends from $m=0$ to $(N_2-1)/2$. For a given value of $m\neq 0$, the basis of the rod is a finite size square unit cell which corresponds to the different values taken by the two indices s_1 and s_2. The cell at $m=0$ has a triangular shape due to the fact that two quanta are indistinguishable. Within this equivalence, the wave function $\Psi_k(s_1,s_2;m)$ associated to the relative distance between the two-vibron excitations, can be viewed as the wave function of the fictitious particle with quasimomentum k. Its dynamics is thus described by a tight-binding Hamiltonian characterized by self energies located on each site and hopping matrices which couple nearest neighbor sites. Both the anharmonicity and the confinement of the monolayer are responsible for the presence of local defects leading to a shift of the self-energies. As shown in Fig. 2(a), the confinement induces the finite size of the different cells and leads to defects located on the contour of these cells. By contrast, the anharmonicity acts onto the triangular cell ($m=0$), only, and leads to an energy shift equal to $-2A$ for the sites belonging to the diagonal (the sites for which $s_1=s_2$).

Although the Schrödinger equation cannot be solved explicitly, we can take advantage of its equivalence with the single particle problem to obtain relevant information on the two quanta dynamics. Such an approach is illustrated in the following section to evaluate the two-vibron Green function.

C. Green function calculation

A useful way to characterize the two vibron dynamics of the confined monolayer is to evaluate the Green function $G=(\omega-H)^{-1}$ associated to the Hamiltonian H. Indeed, the knowledge of the Green function allows us to determine several observables such as the weighted density of states and the spectral response to an external probe. The two vibron density of states $g(\omega)$ is expressed as

$$g(\omega)=-\frac{1}{\pi}\mathrm{Im}\sum_{ls}\sum_{l's'}(l,s;l',s'|G(\omega+io^+)|l,s;l',s'), \quad (13)$$

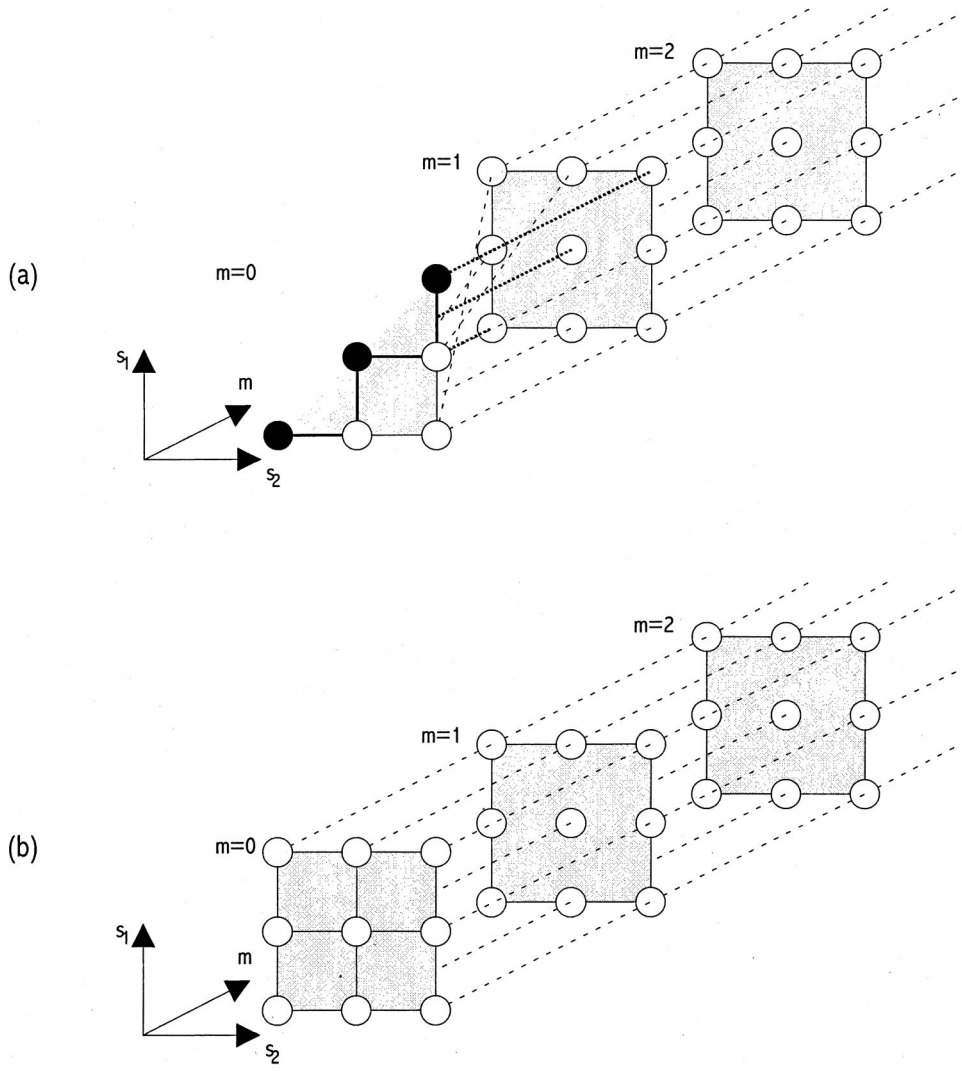

FIG. 2. Equivalence between the Schrödinger equation of the two-vibron states and the dynamics of a single fictitious particle moving quantum mechanically in a three-dimensional lattice. (a) The equivalent lattice, called the real lattice, appears as a finite size, discrete rod with a length which extends from $m=0$ to $m=(N_2-1)/2$. For a given value m, it exhibits a finite size, square unit cell which corresponds to the different values taken by the two indices s_1 and s_2. The cell located at $m=0$ shows a triangular shape instead of a square shape due to the fact that two quanta are indistinguishable. (b) Ideal lattice used to calculate the Green function. The circles define the self frequencies of the sites (s_1,s_2,m) and the lines characterize the hopping constants $\Phi_\perp$ (thin line), $\sqrt{2}\Phi_\perp$ (full line), $\tilde{\Phi}_\parallel(k)$ (dashed line), and $\sqrt{2}\tilde{\Phi}_\parallel(k)$ (dotted line) (see the text).

whereas the two vibron infrared spectrum is proportional to the spectral response $J(\omega)$ defined as

$$J(\omega)=-\frac{1}{\pi}\mathrm{Im}\sum_{ls}\sum_{l's'}(l,s;l,s|G(\omega+io^+)|l',s';l',s'). \tag{14}$$

To calculate the two vibron Green function, we take advantage of the equivalence of the Schrödinger equation and the single particle problem, and use the formalism introduced by Dobrzynski[34] to determine the response function of superlattices and composite materials.

1. General method

To proceed, we first consider the lattice shown in Fig. 2(b) which corresponds to a fully symmetric discrete rod with finite size. It is denoted the ideal lattice by opposition to the real lattice drawn in Fig. 2(a). By comparing Figs. 2(a) and 2(b), it is straightforward to see that $N_1(N_1-1)/2$ sites of the ideal lattice do not belong to the real lattice. We thus define $Q=1-P$ as the projector onto these sites.

Let H_0 denote the tight-binding Hamiltonian which characterizes the dynamics of this ideal lattice. The Hamiltonian H can be obtained by adding an operator V to H_0 and by taking the restriction to the sites which belong to the real lattice as

$$H=P(H_0+V)P. \tag{15}$$

The goal of the operator V, known as the cleavage operator,[34] is first to disconnect in the ideal lattice the sites which do not belong to the real lattice, and then to introduce the real boundary conditions. From Eq. (15), the Green function of the real lattice is thus expressed in terms of the Green function $G_0=(\omega-H_0)^{-1}$ of the ideal lattice, as

$$G=PG_0P+PG_0VP(1-G_0V)^{-1}PG_0P. \tag{16}$$

As a result, assuming that we can solve the Schrödinger equation for the ideal lattice, we are able in principle to compute easily the exact Green function of the real lattice.

2. Dynamics of the ideal lattice

The single particle Schrödinger equation for the ideal lattice is expressed as

$$[\omega_{s_1}+\omega_{s_2}-\omega+\tilde{\Phi}_{\parallel}(k)\Delta_m+\Phi_{\perp}(\Delta_{s_1}+\Delta_{s_2})]\Psi_k^0(s_1,s_2;m)=0, \tag{17}$$

where the appropriate boundary conditions are implicitly used. To solve Eq. (17), we use the method based on the separation of variables and seek for a solution written as

$$\Psi_k^0(s_1,s_2;m)=\phi_1(s_1)\phi_2(s_2)\phi_3(m). \tag{18}$$

Inserting Eq. (18) into Eq. (17) leads to the following system:

$$\begin{aligned}
&-\epsilon_3\phi_3(m)+\tilde{\Phi}_{\parallel}(k)[\phi_3(m+1)+\phi_3(m-1)]=0,\\
&(\omega_{s_2}-\epsilon_2)\phi_2(s_2)+\Phi_{\perp}[\phi_2(s_2+1)+\phi_2(s_2-1)]=0,\\
&(\omega_{s_1}-\epsilon_1)\phi_1(s_1)+\Phi_{\perp}[\phi_1(s_1+1)+\phi_1(s_1-1)]=0,
\end{aligned} \tag{19}$$

where the separated eigenvalues obey the equality $\omega=\epsilon_1+\epsilon_2+\epsilon_3$. As shown by Eq. (19), the separation of the variables reduces the initial problem connected to a three-dimensional lattice to three similar problems related to the propagation of a single particle in a one-dimensional discrete chain. The general solution of each equation in Eq. (19) is expressed as a superimposition of plane waves that propagate in both directions along each chain as

$$\phi_i(x)=A_i^{(+)}e^{iq_ix}+A_i^{(-)}e^{-iq_ix};i=1,2,3, \tag{20}$$

where x stands for m, s_1, and s_2. Because of the finite size of the discrete chains, the values taken by the reduced wave vectors q_i are unknown at this stage. However, substituting Eq. (20) into Eq. (19), leads to a system of equations for the side and core sites of each chain. For the core sites, the solutions satisfy the equations of propagation subjected to the dispersion relations of ideal chains, as

$$\begin{aligned}
&\epsilon_i=\omega_0+2\Phi_{\perp}\cos(q_i);i=1,2,\\
&\epsilon_3=2\tilde{\Phi}_{\parallel}(k)\cos(q_3).
\end{aligned} \tag{21}$$

For the side sites, the system of equations [Eq. (19)] is directly connected to the boundary conditions imposed to each chain. The first equation in Eq. (19) refers to a finite size discrete chain with two free sides. The waves which propagate into such a system are stationary, with a quantization of the wave vector q_3 satisfying to the solution

$$q_3=\frac{p\pi}{L_2}, \tag{22}$$

where $L_2=(N_2+1)/2+1$ and $p=1,2,...,(N_2+1)/2$. By contrast, the second and third equations in Eq. (19) characterize the motion of a single particle confined in a chain containing N_1 sites. The confinement induces specific boundary conditions due to the frequency shifts ω_1 and ω_N with respect to the core frequency ω_0. As shown in previous works,[11,19,20] the allowed values of the wave vectors q_1 and q_2 are the solutions of the equation

$$\frac{(\alpha_1-e^{-iq_i})(\alpha_{N_1}-e^{-iq_i})}{(\alpha_1-e^{iq_i})(\alpha_{N_1}-e^{iq_i})}=e^{2iq_i(N_1-1)}, \tag{23}$$

where $i=1,2$ and $\alpha_{1,N_1}=(\omega_{1,N_1}-\omega_0)/\Phi_{\perp}$. The N_1 solutions of Eq. (23) are either real or complex, depending on the values of the parameters α_1, α_{N_1}, N_1. A real solution for q_i characterizes a stationary wave with a frequency inside the vibron band of the chain. A complex value of q_i leads to the occurrence of a localized mode, with an amplitude strongly localized at the chain sides and a frequency lying below or above the vibron band.

Finally, the Schrödinger equation for the ideal lattice can be solved exactly. Its eigenenergies are given by

$$\omega_k(q_1,q_2,p)=2\omega_0+2\Phi_{\perp}\cos(q_1)+2\Phi_{\perp}\cos(q_2)+2\tilde{\Phi}_{\parallel}(k)\cos\left(\frac{p\pi}{L_2}\right) \tag{24}$$

and the corresponding eigenvectors are expressed as

$$\begin{aligned}
\Psi^0_{k,q_1,q_2,p}(s_1,s_2;m)=A_{q_1,q_2,p}\sin\left(\frac{p\pi(m+1)}{L_2}\right)\\
\times\{\alpha_1\sin[q_1(s_1-1)]-\sin(q_1s_1)\}\\
\times\{\alpha_1\sin[q_2(s_2-1)]-\sin(q_2s_2)\},
\end{aligned} \tag{25}$$

where $A_{q_1,q_2,p}$ is a normalization factor. The ideal Green function is thus written as

$$G_{0,k}(s_1,s_2;m:s_1',s_2';m')=\sum_{p,q_1,q_2}\frac{\Psi^0_{k,q_1,q_2,p}(s_1,s_2;m)\Psi^{0*}_{k,q_1,q_2,p}(s_1',s_2';m')}{\omega-\omega_k(q_1,q_2,p)}. \tag{26}$$

At this step, we have an exact expression for the ideal lattice Green function G_0 [Eq. (26)] which can be used to compute the real lattice Green function as shown in Sec. III C 1 [Eq. (16)]. Note that such a procedure requires the knowledge of the cleavage operator V which can be built straightforwardly by comparing the Schrödinger equations of the real and ideal lattices.

IV. NUMERICAL RESULTS

In this section, we apply the previous formalism to a model monolayer confined between two surface steps. To minimize the number of relevant parameters, we consider a symmetric confinement and assume that the two side molecules exhibit the same frequency redshift, i.e., $\omega_1=\omega_{N_1}=\omega_0-\Delta\omega$, with $\Delta\omega\geqslant 0$. An extension to the general situation with asymmetric blueshifts or redshifts could be done straightforwardly using the same formalism.

The dynamics of the monolayer is studied in two stages. First, we assume that the molecules belonging to adjacent unit cells do not interact ($\Phi_{\parallel}=0$). Such a situation corre-

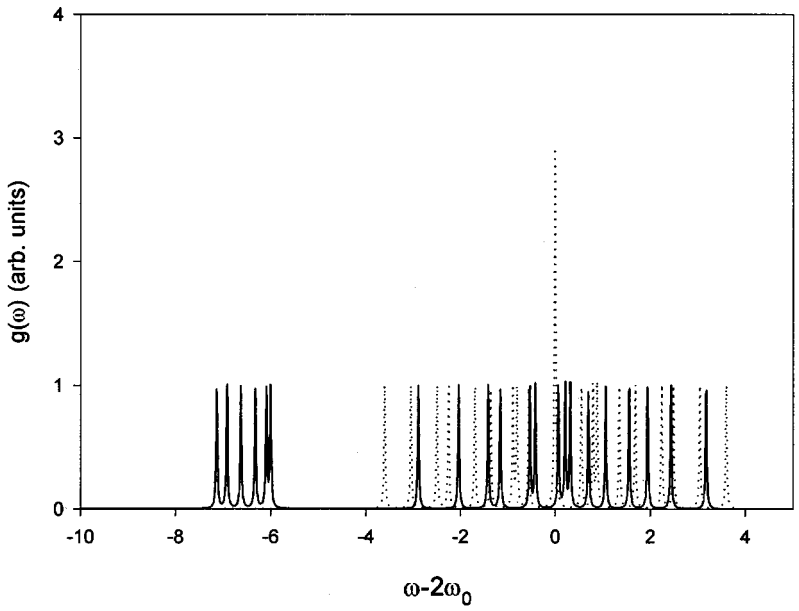

FIG. 3. Density of states $g(\omega)$ in arbitrary unit of a one-dimensional molecular chain formed by $N_1=6$ molecules confined between two symmetric surface steps. Dotted lines and full lines correspond to the density of states of the harmonic chain $(A=0)$ and anharmonic chain $(A=3.0)$, respectively.

sponds to a set of one-dimensional linear chains perpendicular to the steps, the dynamics of which can be analyzed independently. The simplicity of this model allows us to understand the physics of the two-vibron states and the interplay between bound and localized two-vibron states. Then, the two-dimensional confined monolayer is considered. Note that all the numerical calculations are performed using the perpendicular hopping constant $\Phi_\perp$ as frequency unit.

The density of the two-vibron states for a chain formed by $N_1=6$ molecules and two free sides $(\Delta\omega=0)$ is shown in Fig. 3. For a harmonic system $(A=0)$, the density of states

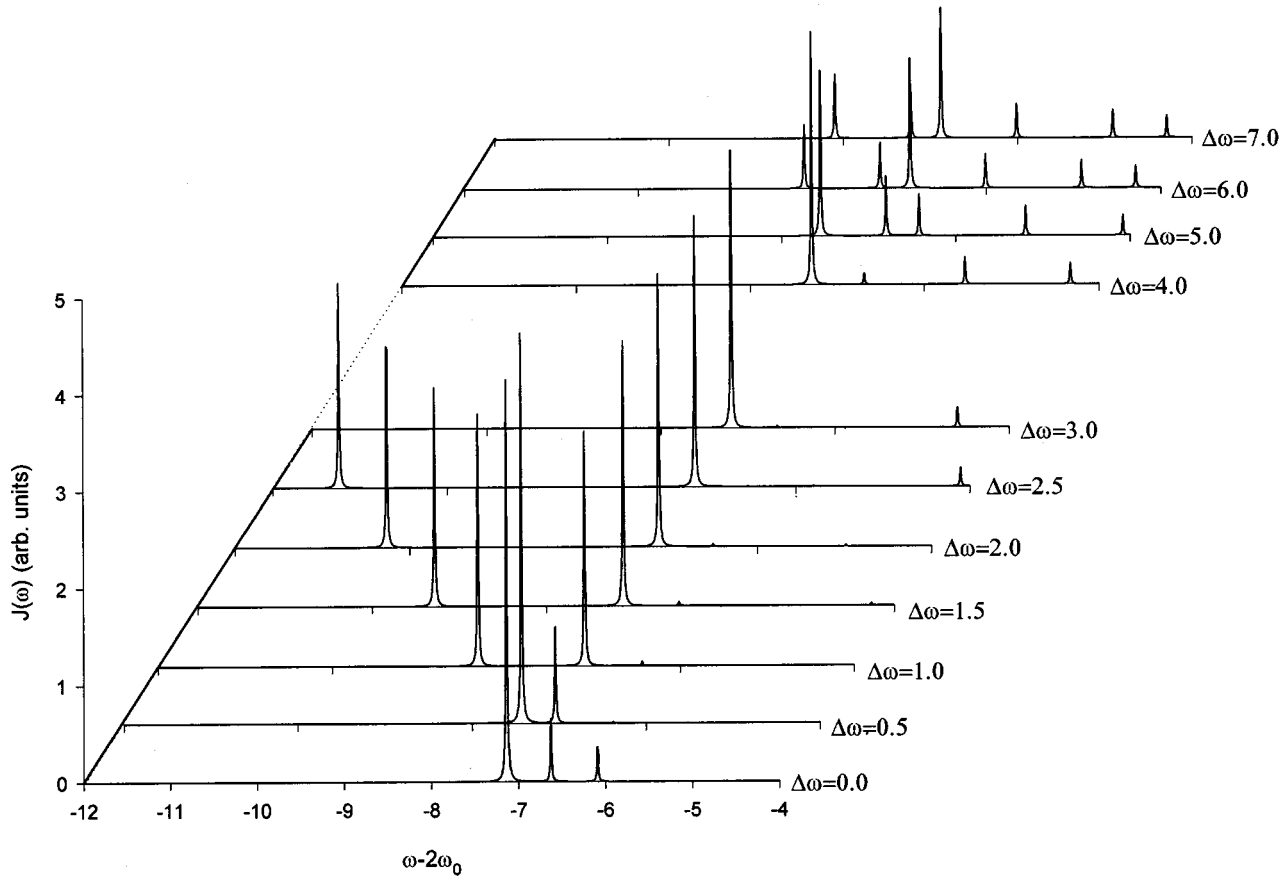

FIG. 4. Behavior of the spectral response $J(\omega)$ in arbitrary unit of a one-dimensional anharmonic $(A=3.0)$ molecular chain $(N_1=6)$ vs the value $\Delta\omega$ of the frequency shift of the two side molecules.

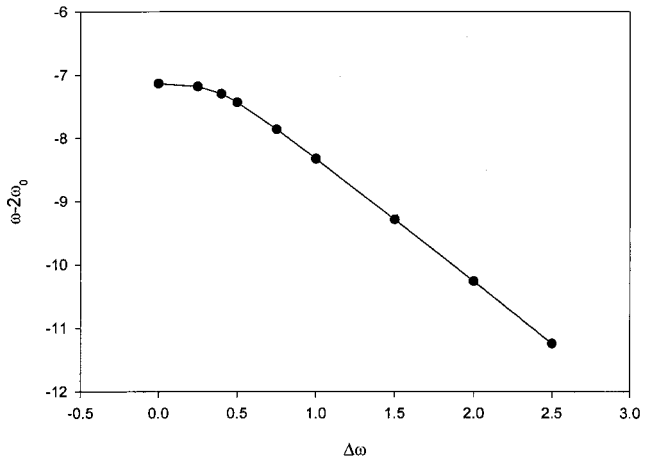

FIG. 5. Behavior of the frequency of the localized two-vibron bound states as a function of the frequency shift $\Delta\omega$ of the two side molecules.

exhibits $N_1(N_1+1)/2=21$ quantum states, the energies of which range between -4.0 and 4.0 around the overtone energy $2\omega_0$ of a single oscillator. Three states are degenerated with a frequency equal to the overtone frequency. This feature is general since $(N_1+1)/2$ states are degenerated in a confined chain with free sides formed by N_1 molecules. For an anharmonic system $(A\neq 0)$, the density of states clearly shows the occurrence of $N_1=6$ states lying outside the previous frequency range since their frequencies are redshifted with respect to the harmonic frequencies. These states correspond to the well-known two-vibron bound states.

To investigate the influence of the frequency shift $\Delta\omega$ of the side molecules on the bound states, the spectral response in the frequency range of the two-vibron bound states is shown in Fig. 4 for an anharmonic parameter equal to $A=3.0$. For $\Delta\omega=0$, the spectral response exhibits three peaks which characterize the response of the optically active bound states. The most intense peak corresponds to the bound state

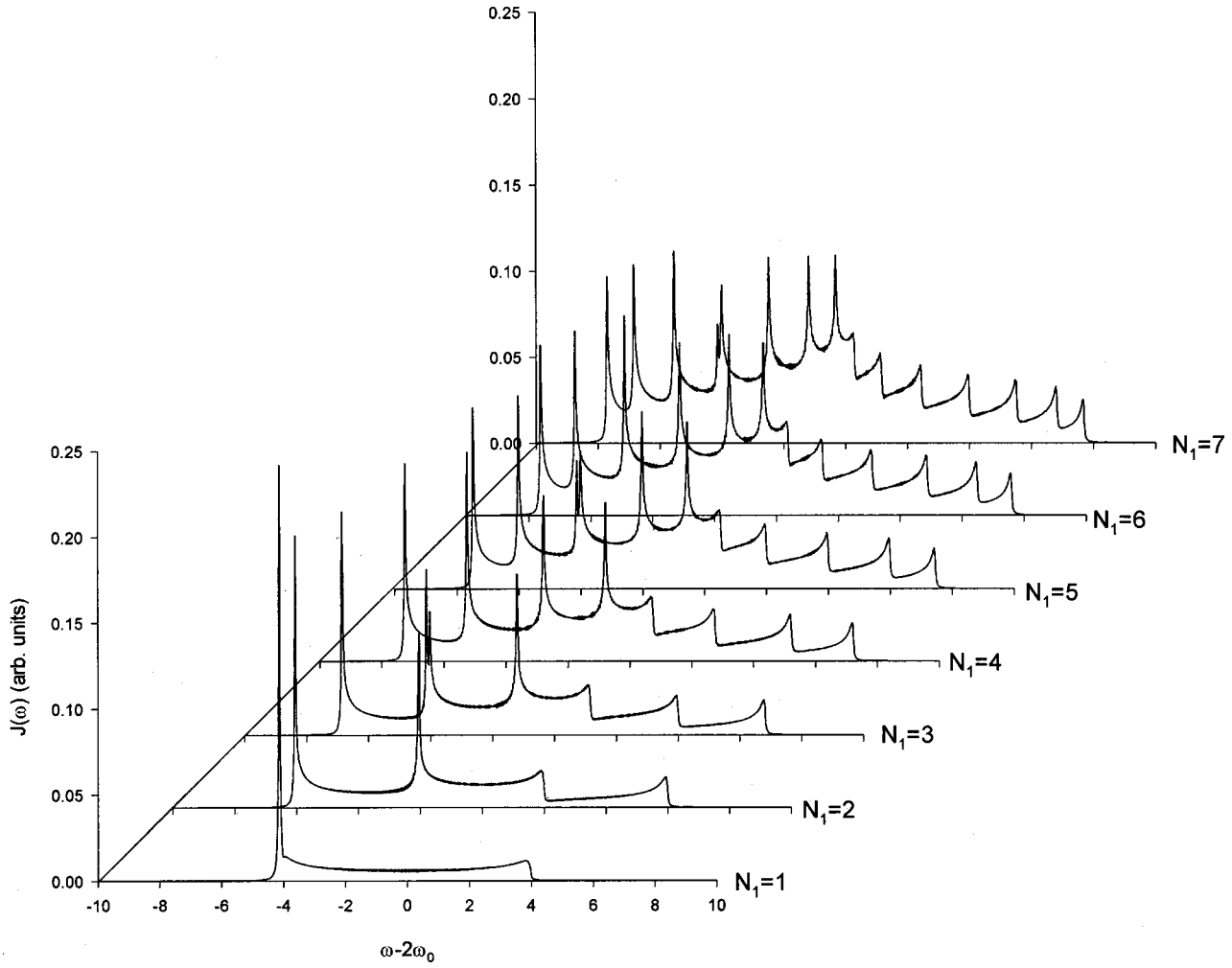

FIG. 6. Behavior of the spectral response of a two-dimensional weakly anharmonic $(A=0.5)$ molecular monolayer as a function of the number of confined molecular rows N_1. The side molecules do not exhibit any frequency shift $(\Delta\omega=0)$.

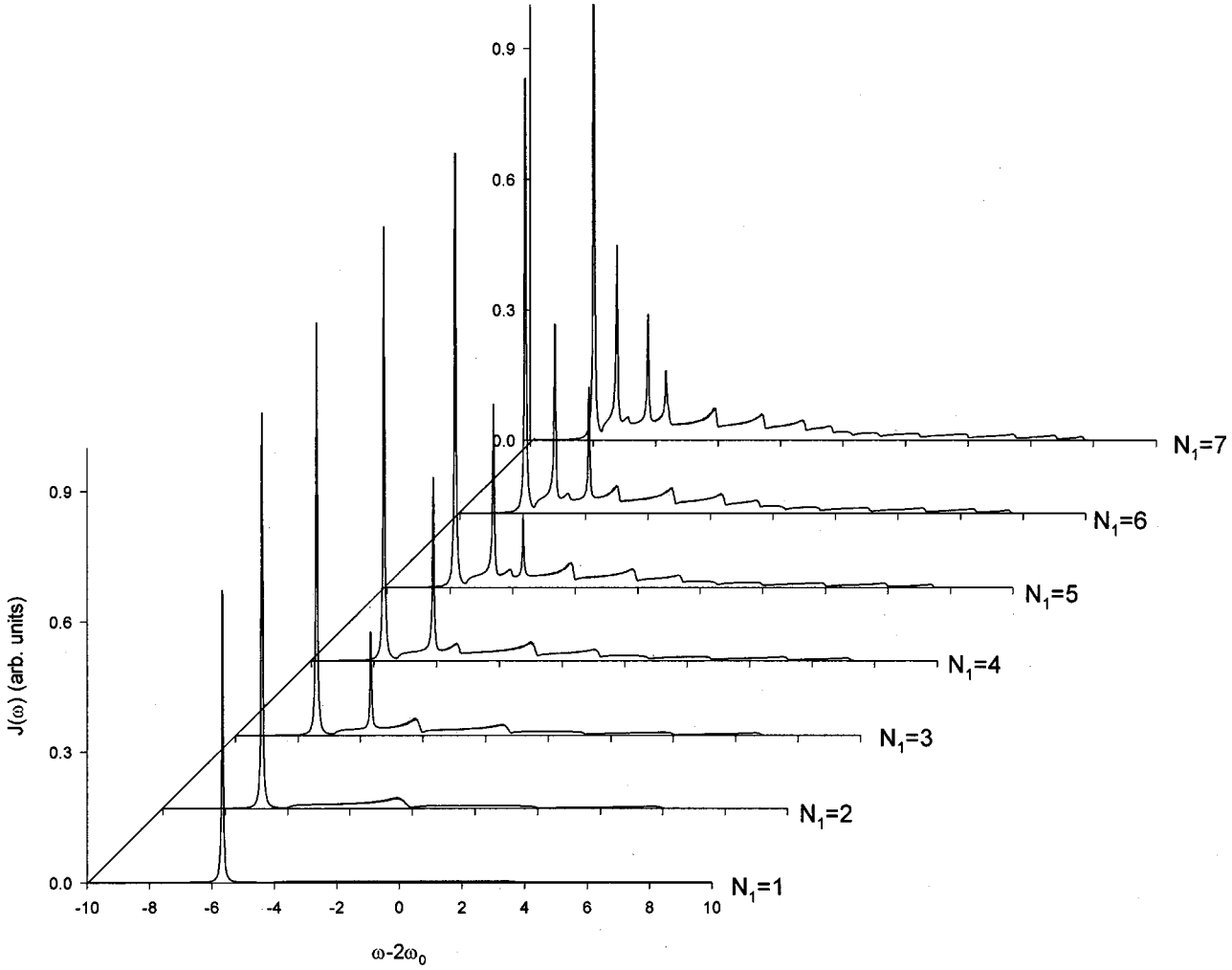

FIG. 7. Behavior of the spectral response of a two-dimensional strongly anharmonic ($A=2.0$) molecular monolayer as a function of the number of confined molecular rows N_1. The side molecules do not exhibit any frequency shift ($\Delta\omega=0$).

with the lower frequency. As the frequency shift $\Delta\omega$ increases, the lowest frequency peak is strongly redshifted whereas another significant peak remains in the frequency range of the bound states. As shown in Fig. 5, the position of the lowest frequency peak slightly decreases as $\Delta\omega$ increases and shows a linear dependence, with a more abrupt slope when $\Delta\omega$ becomes greater than 0.5. As $\Delta\omega$ increases up to 3.0, there is no significant change in the spectral response. However, for larger $\Delta\omega$ values, a more complicated structure occurs with several peaks and a strong splitting of the initially unshifted peak takes place for $\Delta\omega\approx 6.0$.

For the two-dimensional monolayer, the behavior of the spectral response with respect to the size N_1 of the confinement is shown in Figs. 6 and 7 for two different values of the anharmonic parameter *A*. The calculations are performed by assuming isotropy of the lateral interactions ($\Phi_{\parallel}=\Phi_{\perp}$). For a low anharmonicity (Fig. 6) corresponding to $A=0.5$, a broad band centered on the overtone $2\omega_0$ of a single oscillator occurs. The shape of the band is slightly asymmetric with respect to the overtone frequency with intense low frequency peaks. Its width increases as the number N_1 of confined molecules par unit cell increases and clearly converges to a limit which is rapidly reached when N_1 is greater than 4. For a given value of N_1, the spectral response displays $2N_1$ maxima. The low frequency part of the band shows N_1 intense peaks while the high frequency part exhibits N_1 maxima with a much lower intensity. As the anharmonicity increases, the shape of the spectral response is modified. Indeed, for $A=2.0$, the band asymmetry and the low frequency peak intensity are enhanced, while the features in the high frequency part disappear. The resulting spectral response exhibits a finite set of intense peaks with a lower frequency than the overtone $2\omega_0$. Whatever the size of the confinement, the intensity of the peaks decreases as their frequency shifts towards the overtone value $2\omega_0$. The frequency of the most intense peak is redshifted as N_1 increases and reaches a limited value when N_1 becomes greater than 4. The number of remaining peaks is equal to the integer part of $(N_1+1)/2$. For instance, there are one peak for both $N_1=1$ and 2 and two peaks for $N_1=3$ and 4.

The influence of the anisotropy of the lateral interactions is shown in Fig. 8 for $N_1=2$ confined molecular rows and for a weak anharmonicity ($A=0.3$). When $\Phi_{\parallel}=0.3\Phi_{\perp}$

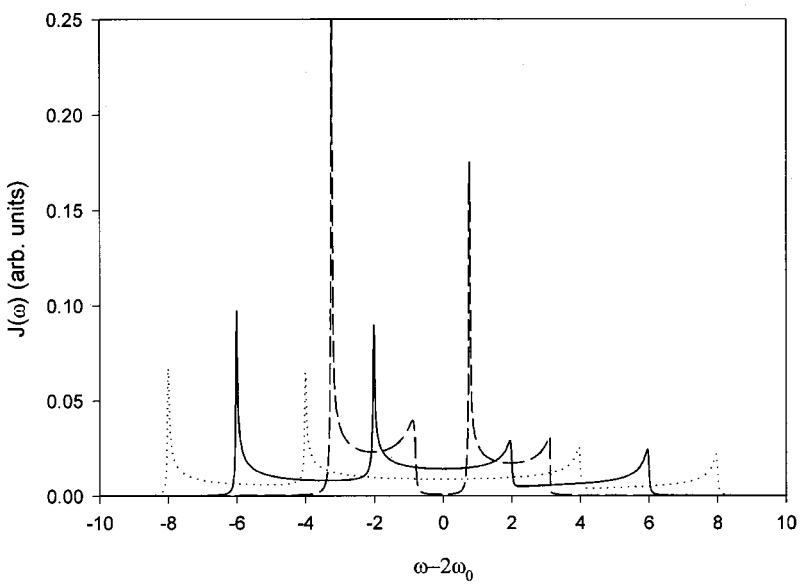

FIG. 8. Behavior of the spectral response of a weakly anharmonic ($A=0.3$) confined layer formed by $N_1=2$ molecular rows as a function of the lateral hopping constant $\Phi_\parallel$. Three different situations are illustrated corresponding to $\Phi_\parallel=0.3\Phi_\perp$ (dashed line), $\Phi_\parallel=\Phi_\perp$ (full line), and $\Phi_\parallel=1.5\Phi_\perp$ (dotted line), respectively. The side molecules do not exhibit any frequency shift ($\Delta\omega=0$).

(dashed line), the spectral response is formed by two distinct bands located on both sides of the overtone frequency $2\omega_0$. These bands have the same width and exhibit a similar shape with a single intense peak. As the lateral coupling $\Phi_\parallel$ increases, the width of the two bands increases and their overlap takes place when $\Phi_\parallel \approx 0.5\Phi_\perp$. For larger values of $\Phi_\parallel$ (full and dotted line), the spectral response exhibits a single band which the characteristics have been discussed previously. The width of this single band increases as $\Phi_\parallel$ increases.

The symmetric confinement of strongly anharmonic molecules ($A=3.0$) is illustrated in Fig. 9, for two different values $N_1=5$ and $N_1=6$ of the size of confinement. The internal frequency of the side molecules is assumed to be redshifted identically and is equal to $\omega_0-\omega_{1,N_1}=\Delta\omega=2.0$. In both cases, the spectral response exhibits two intense peaks as expected from the previous rule. The lowest frequency peak, which is the most intense, appears to be isolated from the second peak which belongs to the tail of the broad band. As shown in Fig. 9, the frequency and the intensity of the most intense peak do not depend on the even or odd number of confined molecular rows. By contrast, the intensity of the second peak increases by a factor 2 and its frequency is slightly redshifted as the size of confinement varies from $N_1=5$ to $N_1=6$.

V. DISCUSSION

To interpret the features observed for the one-dimensional confined chain, let us remind that the Schrödinger equation for the two-vibron states is equivalent to the single particle problem on the three-dimensional lattice shown in Fig. 2(a). Since $\Phi_\parallel=0$, this lattice reduces to the two-dimensional triangular cell located at $m=0$. Within this picture, the bound states correspond to localized states occurring in the vicinity of the defects associated to the anharmonic effects, i.e., the

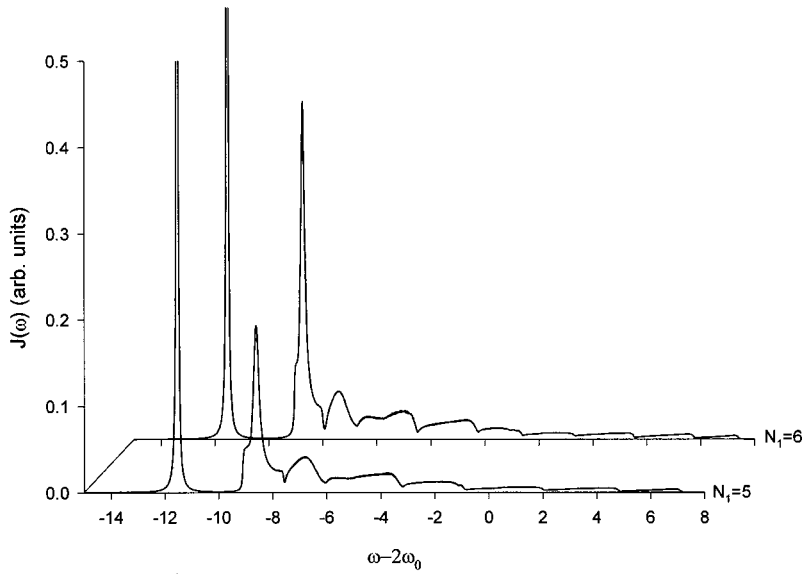

FIG. 9. Behavior of the spectral response of a two-dimensional strongly anharmonic ($A=3.0$) monolayer vs the number of confined molecular rows. The two side molecules exhibit the same frequency shift equal to $\Delta\omega=2.0$.

defects located on the diagonal of the lattice for which $s_1 = s_2$. In other words, for a reasonably strong anharmonicity, i.e., $A > \Phi_\perp$, these N_1 sites, with a self-frequency equal to $2\omega_0 - 2A$, are decoupled from the free sites which have a self-frequency equal to the overtone $2\omega_0$. However, an effective interaction occurs between these N_1 sites via high order processes involving the free sites. This interaction leads to the splitting of the frequencies of the bound states. To illustrate this feature we use a second order perturbation theory to calculate the effective coupling Φ_e between the sites (s_1, s_1) and (s_1+1, s_1+1) mediated by site (s_1, s_1+1). We find that $\Phi_e = -\Phi_\perp^2/A$.

In addition to the defects due to the anharmonicity, the frequency shift of the side molecules due to the confinement is responsible for the occurrence of defects distributed over the contour of the triangular cell. As a result, the restricted one-dimensional chain exhibits also two defects located on the side sites $s_1 = s_2 = 1$ and $s_1 = s_2 = N_1$. These two defects are responsible for the occurrence of localized two-vibron bound states characterized by a wave function which is strongly localized on sites $s_1 = s_2 = 1$ and $s_1 = s_2 = N_1$. As shown in Fig. 4, the spectral signature of these localized bound states corresponds to the lower frequency peak which the frequency depends on the shift $\Delta\omega$. From a mathematical point of view, this process can be formulated by restricting the Schrödinger equation of the triangular cell to the sites located on the diagonal. Therefore, the second order reduced Schrödinger equation for the wave function $\Psi_s = \Psi_k(s, s, m = 0)$ is expressed as

$$[2\omega_0 - 2A + \delta\omega(\delta_{s,1} + \delta_{s,N_1}) - \omega]\Psi_s - \Phi_e(\Psi_{s+1} + \Psi_{s-1}) = 0, \tag{27}$$

where $\delta\omega = -2\Delta\omega + \Phi_e$. By applying the renormalization group theory used in previous papers to solve similar equations,[11,19] it is straightforward to show that Eq. (27) exhibits two localized solutions which occur for two critical values of the parameter $\Delta\omega$ equal to

$$\Delta\omega^* = \frac{\Phi_\perp^2}{2A}\left(2 + \frac{1 \pm 1}{N_1 - 1}\right). \tag{28}$$

This relation can be compared with the results obtained in Ref. 11 since it was shown that localized single-vibron states in a confined chain occur for critical values $\Delta\omega^* = \Phi_\perp[1 + (1 \pm 1)/(N_1 - 1)]$. As a result, Eq. (28) shows that a strong anharmonicity enhances the occurrence of localized states by softening the critical values ($\Delta\omega^* \approx \Phi_\perp^2/A$ instead of $\Delta\omega^* \approx \Phi_\perp$). The localization corresponds in fact to a competition between the lateral coupling which tends to delocalize the excitations and the frequency shift of the side molecules which tends to localize these excitations. In an anharmonic molecular chain, a strong anharmonicity leads to the formation of bound states which are the superimposition of states formed by two quanta located on the same molecule. Since the effective lateral interaction between these latter states is strongly reduced by the anharmonicity, two situations can occur. First, localized two-vibron bound states can be obtained even if there is no localized single-vibron states. Second, if the frequency shift of the side molecules is sufficient to localize single-vibron states, then the localization of the two-vibron bound states will be still stronger than the localization of the single-vibron state.

As shown in Fig. 4, the defects induced by the frequency shift of the side molecules are also responsible for other phenomena. Indeed, when $\Delta\omega$ increases to reach a value of about the anharmonic shift $2A$, a resonance occurs. More precisely, a resonant coupling takes place between the sites $s_1 = 2$, $s_2 = 2$ and $s_1 = 1$, $s_2 = 2$ and between the sites $s_1 = N_1 - 1$, $s_2 = N_1 - 1$, and $s_1 = N_1 - 1$, $s_2 = N_1$. Basically, such a coupling involves a two-vibron bound state and a state formed by the pair of a single-vibron localized either on the site $s = 1$ or $s = N_1$ and a free vibron. This resonance is responsible for the breaking of the bound between two vibrons induced by the anharmonic interaction. As a result, the eigenstates appear as a superimposition of both kinds of states which leads to the occurrence of several peaks in the spectral response.

In a two-dimensional confined monolayer, the same features are observed although the signature of theses features in the spectral response can appear in a different way. As for the one-dimensional chain, the shape of the spectral response gives information on the occurrence of localized modes induced by the frequency shift of the side molecules. Indeed, the lowest frequency peak characterizes the spectral response of localized two-vibron bound states. Although the frequency and the intensity of this peak do not depend on the size of the confinement, its occurrence involves in a complicated way the different dynamical parameters. Due to the symmetric confinement, there are two localized two-vibron bound states, which correspond to the localization of two vibrons onto the two side molecules. Within the strong anharmonicity limit, the second order perturbation expansion can be used to determine an approximate value of the frequency of the localized two-vibron bound state. Indeed, using the lattice picture shown in Fig. 2(a), the renormalized self-energy of the side site $(s_1 = 1, s_2 = 1, m = 0)$ corresponds to its interaction with its two nearest neighbors located in the cells $m = 0$ and $m = 1$, respectively. As a result, the frequency of the localized two-vibron states is approximated as

$$\omega_L \approx 2\omega_0 - 2\Delta\omega - 2A - \frac{2}{2A + \Delta\omega}(\Phi_\perp^2 + 4\Phi_\parallel^2). \tag{29}$$

As shown in Figs. 6–9, the line shape of the two-vibron spectral response appears to be very sensitive to the structure of the monolayer. Especially, this shape strongly depends on the number of confined rows through the number of intense peaks in $J(\omega)$. Such a feature indicates that infrared spectroscopy applied to the two-vibron response of a confined monolayer can provide valuable information on the nanostructuration of molecular rows at the steps of a vicinal surface. This is a remarkable feature which adds to the information brought by the usual one vibron response.[16] At low anharmonicity, the number of observed intense peaks is equal to the number N_1 of confined rows as shown in Fig. 6. At strong anharmonicity, the number of intense peaks is the

integer part of $(N_1+1)/2$ (Fig. 7). In this latter case, the ambiguity over the corresponding odd or even number of rows can be removed by comparing the relative intensity of the peaks. Since the width of the spectral band depends on the size of confinement, row-by-row growth of molecular monolayer close to substrate steps could be followed using infrared spectroscopy.

In addition, the fact that the shape of $J(\omega)$ is also very dependent on the parameters characterizing the vibron dynamics, especially the lateral hopping constants, the anharmonicity coefficient and the frequency shift due to adsorption of molecules on step sites rather than on terrace sites, data on the two-vibron spectroscopy could be used as a probe of such parameters. Indeed, the width of $J(\omega)$ is directly connected to the lateral interaction between molecules belonging to adjacent rows and it gives information on the interaction process through the hopping constant $\Phi_\perp$. Moreover, the profile of $J(\omega)$, especially the relative positions of the peaks in the spectrum, depends on the relative values of $\Phi_\perp$ and $\Phi_\parallel$, and is thus an indirect probe of the anisotropy of the interactions in the confined monolayer. Last, the frequency of the peaks connected to localized two-vibron bound states can be used as an additional probe of the various dynamical parameters in the strong anharmonicity limit, using Eq. (29). These results corroborate the recent results obtained by Jakob[30] who has demonstrated the ability of infrared spectroscopy to study vibrational band structures in adsorbates by exciting the two-vibron states.

In a general way, the relative values of the different dynamical parameters do not follow well-defined rules and several situations can occur depending on the nature of both the adsorbate and the substrate. Indeed, when the molecules are adsorbed close to the steps of a metal surface, their internal frequencies are either redshifted or blueshifted with respect to their values on a terrace. For instance, the frequency of the stretch vibration for the system CO/Pt(111) is redshifted by about 20–30 cm^{-1} (Ref. 30) whereas the presence of steps for the system CO/Cu(100) (Ref. 35) leads to a blueshift of about 15 cm^{-1} of the internal vibration frequency of the side molecules. The anharmonicity of small molecules on metal surfaces is usually close to the gas phase anharmonicity (typically of about $A=10-20\,cm^{-1}$ for CO and NO) and appears strong enough to induce two-vibron bound states. Therefore, we can expect the occurrence of localized two-vibron bound states when confining such molecules on a vicinal surface. However, as pointed out by Jakob,[30] this no longer the case for the system Ru(001)-(2×1)-(O+NO), for which the lateral coupling is stronger than the anharmonicity ($A\approx 0.6\times\Phi_\perp$) and prevents the occurrence of bound states. This latter case illustrates the theoretical situation considered in Fig. 6. Although CO and CO_2 adsorption on ionic surfaces was shown to be different on steps and terraces,[36] no experiment has clearly characterized the frequency shift of their internal vibrations. However, it has been shown from theoretical calculations that adsorption of CO_2 close to ionic surface steps leads to a redshift $\Delta\omega$ of the frequency of the asymmetric stretching mode equal to 9 cm^{-1} on NaCl and to 3 cm^{-1} on MgO.[36] Similar results for CO are expected. For the (2×1) CO monolayer adsorbed on NaCl, the lateral interaction was shown to be strongly anisotropic with a vibron bandwidth equal to 3 cm^{-1} along the longer size of the unit cell and to 12 cm^{-1} along the perpendicular direction.[32] Assuming an anharmonic parameter equal to the gas phase parameter ($A=13\,cm^{-1}$), a strong anharmonicity together with a strong anisotropy in the vibron propagation characterizes such a system and we thus expect the formation of localized two-vibron bound states close to the steps. Such a situation is illustrated in Figs. 7 and 9. For the hydrogen-terminated vicinal Si surfaces, the steps were shown to induce a strong modification of the vibron dynamics leading to a frequency blue-shift which ranges from 11 to 52 cm^{-1}.[14–17] For this system, the lateral interaction is very small, leading to a vibron dispersion of about 10 cm^{-1} while the anharmonicity was found to be close to that of the gas phase value, i.e., $A=34\,cm^{-1}$.

To conclude, let us mention first that infrared-visible sum frequency generation (SFG) spectroscopy should in principle provide still a more clear signature of the peaks in the spectral profile than conventional linear infrared spectroscopy. Indeed, the fact that the intensity of peaks in SFG spectrum depends on the square modulus of the nonlinear susceptibility tends to enhance the most intense peaks at the expense of the broad structure. Since the detection of two-vibron bands is not currently a straightforward experimental task, SFG data should therefore be an additional help to the peak assignment. However, such a detection in linear and nonlinear spectroscopy rests on the broadening of the peaks. Let us remind that the present approach has been carried out by disregarding the dynamical influence of the external modes of the monolayer (translational and orientational motions) and of the substrate (phonon dynamics). Jakob and Persson have shown[31] that the energy relaxation rate for the two-vibron states is twice the rate connected to the energy relaxation of a single vibron. Moreover, the dephasing constant of the two-vibron states is about 4 times the single-vibron dephasing constant. As a result, dephasing and population relaxation could appreciably modify the infrared signals by inducing dynamical frequency shift and broadening of the peaks. At low temperature, these dynamical effects should remain small but increasing the temperature would require to describe the influence of the relaxation mechanism on the spectral response of a confined monolayer in a more sophisticated theoretical formalism.

[1] *The First Thirty Years* (special issue), edited by C.B. Duke [Surf. Sci. **299/300**, 1 (1994)], and references therein.

[2] N. Sundaram, S.A. Chalmers, P.F. Hopkins, and A.C. Gossard, Science **254**, 1326 (1991).

[3] P. Gambardella, M. Blanc, H. Brune, K. Kuhnke, and K. Kern, Phys. Rev. B **61**, 2254 (2000).

[4] G. Meyer and K.H. Rieder, Surf. Sci. **377–379**, 1087 (1997).

[5] G. Binnig and H. Rohrer, Rev. Mod. Phys. **71**, S324 (1999).

[6] G. Dujardin, R.E. Walkup, and Ph. Avouris, Science **255**, 1232 (1992).
[7] J. Gaudioso, H.J. Lee, and W. Ho, J. Am. Chem. Soc. **121**, 8479 (1999).
[8] H.J. Lee and W. Ho, Phys. Rev. B **61**, R16 347 (2000).
[9] L.J. Lauhon and W. Ho, Surf. Sci. **451**, 219 (2000).
[10] V. Pouthier, J.C. Light, and C. Girardet, J. Chem. Phys. **114**, 4955 (2001).
[11] V. Pouthier and C. Girardet, Surf. Sci. (to be published).
[12] H.C. Chang and G.E. Ewing, J. Electron Spectrosc. Relat. Phenom. **54/55**, 39 (1990).
[13] C. Tegenkamp, W. Ernst, M. Eichmann, and H. Pfnur, Surf. Sci. **466**, 41 (2000).
[14] M. Morin, P. Jakob, N.J. Levinos, Y.J. Chabal, and A.L. Harris, J. Chem. Phys. **96**, 6203 (1992).
[15] K. Kuhnke, M. Morin, P. Jakob, N.J. Levinos, Y.J. Chabal, and A.L. Harris, J. Chem. Phys. **99**, 6114 (1993).
[16] P. Jakob, Y.J. Chabal, K. Raghavachar, and S.B. Christman, Phys. Rev. B **47**, 6839 (1993).
[17] K. Kuhnke, A.L. Harris, Y.J. Chabal, P. Jakob, and M. Morin, J. Chem. Phys. **100**, 6896 (1994).
[18] P. Guyot-Sionnest, P. Dumas, Y.J. Chabal, and G.S. Higashi, Phys. Rev. Lett. **64**, 2156 (1990).
[19] V. Pouthier and C. Girardet, J. Chem. Phys. **112**, 5100 (2000).
[20] V. Pouthier, C. Ramseyer, and C. Girardet, Surf. Sci. **382**, 349 (1997); **400**, 176 (1998).
[21] A.S. Davydov and N.I. Kisluka, Phys. Status Solidi **59**, 465 (1973); Zh. Eksp. Teor. Fiz **71**, 1090 (1976) [Sov. Phys. JETP **44**, 571 (1976)].
[22] S. Aubry, Physica D **103**, 201 (1997).
[23] A. J. Sievers and S. Takeno, Phys. Rev. Lett. **61**, 970 (1988).
[24] J.C. Kimball, C.Y. Fong, and Y.R. Shen, Phys. Rev. B **23**, 4946 (1981).
[25] A.C. Scott, J.C. Eilbeck, and H. Gilhoj, Physica D **78**, 194 (1994).
[26] P. Guyot-Sionnest, Phys. Rev. Lett. **67**, 2323 (1991).
[27] R.P. Chin, X. Blase, Y.R. Shen, and S.GT. Louie, Europhys. Lett. **30**, 399 (1995).
[28] P. Jakob, Phys. Rev. Lett. **77**, 4229 (1996).
[29] H. Okuyama, T. Ueda, T. Aruga, and M. Nishijima, Phys. Rev. B **63**, 233404 (2001).
[30] P. Jakob, J. Chem. Phys. **114**, 3692 (2001).
[31] P. Jakob and B.N.J. Persson, J. Chem. Phys. **109**, 8641 (1997).
[32] V. Pouthier, P. Hoang, and C. Girardet, J. Chem. Phys. **110**, 6963 (1999).
[33] V. Pouthier and C. Girardet, Phys. Rev. B **60**, 13 800 (1999).
[34] L. Dobrzynski, Surf. Sci. **299/300**, 1008 (1994).
[35] E. Borguet and H.L. Dai, J. Chem. Phys. **101**, 9080 (1994).
[36] S. Briquez, A. Lakhlifi, S. Picaud, and C. Girardet, Chem. Phys. **194**, 65 (1995).